LBL--18777

DE85 006590

Invited paper presented at the 7th High Energy Heavy Ion Study, GSI, W. Germany, October 8-12, 1984

COPLANARITY OF TWO-PROTON EMISSIONS IN 400 MeV/nucleon Ne + NaF, Pb REACTIONS

Isao TANIHATA

Institute for Nuclear Study, University of Tokyo,
3-2-1 Midori-cho, Tanashi, Tokyo 188, JAPAN

and

Lawrence Berkeley Laboratory, University of California
Berkeley, California 94720, USA

Abstract

Two-proton coincidence spectra have been measured in a wide kinematical range for ^{20}Ne + NaF and ^{20}Ne + Pb collisions at 400 MeV/nucleon. Coplanar-type correlations show different feature between Ne+NaF and Ne+Pb target reactions. A strong in-plane correlation, which correspond to quasi-elastic scatterings(QES) of nucleons, was observed in wide angular range(15-90°) in NaF target collisions. Angular distributions of QES were reproduced reasonably well by a single nucleon-nucleon scattering model. Enhancement of the QES at momentum transfer around t=2-3m_π, which is predicted as an indication of pionic instability, was not observed. In Ne+Pb collisions, an azimuthally asymmetric emission of particles with respect to the beam axis were implied by the anti-coplanar correlation. A new type of coplanar correlation between the emission angle and the momentum suggests a back-to-back emission of projectile and target nucleons.

1. Introduction

Two-particle coincidence measurements at a large relative momentum have shown to provide unique information for understanding the reaction mechanism of high-energy nuclear collisions.[1,2] The previous measurements on heavy-ion collisions, which had a coincidence counter only at 40°, showed distinct difference between a light nucleus-nucleus collision and a light and heavy nucleus-nucleus collision. In collisions between light nuclei such as C + C, Ne + NaF, and Ar + Ar, two-proton emissions show a strong in-plane correlation which is consistent with quasi-elastic scatterings(QES) between nucleons. In collisions with heavy target, on the other hand, out-of-plane emissions of two-protons were observed to be much stronger than in-plane emissions. It suggested an azimuthally asymmetric emission of the protons with respect to the beam axis.

Gylassy and Greiner[3] predicted that an enhancement of QES cross sections would be seen if pionic instability or condensation is achieved in the heavy-ion collisions. Under the prediction, the enhancement is expected at momentum transfer(t) around 2-3m_π which correspond to an emission angle around 20-30° for 400 MeV/nucleon collisions. In the present measurement we covered a wide angular range , namely from 12 to 90°, so that we could observe the angular distribution of QES.

Recently, asymmetric emissions of light particles were observed in reactions between Nb + Nb by the plastic ball experiment.[4] They suggested that the preferential angle of particle emission depend on the impact parameter of the collision. These asymmetric emissions, observed in two-particle correlations and in the plastic-ball experiment, was firstly considered as a hint of the hydro-dynamical behavior in heavy ion collisions mainly because that cascade models could not predict the asymmetry. If a hydro-dynamical model is assumed to describe heavy-ion collisions correctly, it almost ensures from these observed asymmetry that a highly compressed matter is produced during collisions. Recent development of cascade models,[6,7,8] however, showed that the asymmetric emission of particles are also reproduced within their frame work. Therefore we are, again, back to the state that we have to fined out which is

the most appropriate model to describe heavy-ion collisions.

In a two-particle coincidence measurement, a good statistics can be obtained so that even a weak correlation between momenta and angles of two particles could be seen. In the present experiment, we have measured two-proton correlations in a wide angular and momentum range in order to obtain data which could serve as a good test ground of various models. Measurements were made for two protons emitted in same reaction plane(in-plane; see Fig. 1a) and for two protons emitted in different reaction planes perpendicular with each other(out-of-plane; see Fig. 1b). In the next section brief description of experimental system is shown. Data obtained in ^{20}Ne+NaF collisions are shown in section 3. Data of ^{20}Ne+Pb collisions are discussed in section 4.

2. Experimental System

Two-proton inclusive reactions,

$$^{20}\mathrm{Ne} + \mathrm{A} \rightarrow p_1 + p_2 + \mathrm{X} \quad , \tag{1}$$

were measured at 400 MeV/nucleon. Figure 2 shows the experimental setup used in the present experiment. A beam of 400 MeV/nucleon Ne accelerated by Bevalac was used. Particles emitted from the target were detected by a magnetic spectrometer(SP) and four sets of time-of-flight(TOF) counter telescopes(RF, RC, UF, and UC). The magnetic spectrometer was the same one as used in previous measurements,[1,2] so that no further description is given here. Each TOF counter consisted of three plastic scintillation counters. Last scintillators of TOF counters were connected to two photo-tubes located at both ends so that the positions of the particles were determined. Two forward telescopes(RF and UF) covered scattering angles from 15° to 45°, and two other telescopes(RC and UC) covered from 45° to 90°. The relative azimuthal angle($\Delta\phi$) between SP and RF(or RC) was 180°, and that between SP and UF(or UC) was 90°. The TOF counters detected particles with momentum larger than 250 MeV/c. A particle identification could not be made in TOF counters except the separation of charges. All Z=1 particles detected in TOF counters were treated as protons. The largest mixture of particles was deuterons which could be estimated from SP data where particle separation was excellent. Effect of deuteron and other particles to the two-particle correla-

tion functions are estimated to be very small.

The spectrometer(SP) covered the proton momentum between 450 MeV/c to 1500 MeV/c. Angular setting of SP were 12, 15, 20, 25, 30, 40, 45, 50, 60, 75, and 90 degrees.

In-plane two-particle cross sections

$$\sigma_{in}(P_1,\theta_1,P_2,\theta_2) = \frac{d\sigma^4(P_1,\theta_1,P_2,\theta_2,\Delta\phi=\pi)}{dP_1 d\Omega_1 dP_2 d\Omega_2} \tag{2}$$

and out-of-plane two-particle cross sections

$$\sigma_{out}(P_1,\theta_1,P_2,\theta_2) = \frac{d\sigma^4(P_1,\theta_1,P_2,\theta_2,\Delta\phi=\pi/2)}{dP_1 d\Omega_1 dP_2 d\Omega_2} \tag{3}$$

were determined from coincidence measurements between SP and TOF counters. In the equation as well as in the discussion hereafter, the subscript 1 is used for a particle detected by SP and 2 is for a particle in a TOF counter. The single particle inclusive cross sections were also measured simultaneously so as to eliminate possible systematic errors due to the differences in solid angles and any inefficiencies of the detectors.

3. Ne + NaF Data

Contour lines in Figs.3, 4, and 5 show the coplanar correlation function, $C(P_1,\theta_1)$, deduced from two-proton coincidence cross sections;

$$C(P_1,\theta_1) = \frac{\int \sigma_{in}(P_1,\theta_1,P_2,\theta_2)dP_2 d\Omega_2}{\int \sigma_{out}(P_1,\theta_1,P_2,\theta_2)dP_2 d\Omega_2} . \tag{4}$$

The region of the integration for momentum and angle are shown by a shadowed area in each figure. The value of $C(P_1,\theta_1)>1$ indicates that more particles are emitted in the same reaction plane, and $C(P_1,\theta_1)<1$ indicates that more particles are emitted in one azimuthal side of the beam axis(see Fig. 6). Kinematical locus of nucleon-nucleon QES is also shown by a solid line in the figures.

When coincidence protons(p_2) were detected on the QES kinematics, as shown in Fig.3e and Fig.4c, strong peaks in $C(P_1,\theta_1)$ ($\approx$1.4) are seen on the QES kinematic circle right opposite to the hatched area. The correlation $C(P_1,\theta_1)$ thus shows a dominance of QES. When p_2 was detected inside QES circle(Fig.3d), the correlation is weak $C(P_1,\theta_1)\approx$1.

For p_2 outside QES circle (Fig.3f and Fig.4d), $C(P_1,\theta_1)$ shows general tendency that it is larger for larger transverse momentum(P_T), i.e. protons with large P_T are associated more by large P_T protons on the opposite side.

In order to see the QES angular distributions more quantitatively, difference of in-plane to out-of-plane coincidence cross sections,

$$\Sigma_d = \frac{d^2\sigma_d(\theta_1,\theta_2)}{d\Omega_1 d\Omega_2} = \int \sigma_{in}(P_1,\theta_1,P_2,\theta_2)dP_1dP_2 - \int \sigma_{out}(P_1,\theta_1,P_2,\theta_2)dP_1dP_2 \quad . \tag{5}$$

was calculated. To select QES components, integration on P_1 and P_2 was made under the restriction that the sum energy of two protons ($E_s=E_1+E_2$) lies between 300 to 500 MeV. Figure 7 shows the results of differences of cross sections. Solid curves in the figure show results of single nucleon-nucleon scattering calculations which includes a Gaussian-type momentum distribution, ($\exp(-P^2/2\alpha^2)$), of nucleons inside the nucleus. Width of the Gaussian α=108 MeV/c was used, which corresponds to a Fermi momentum of 240 MeV/c. This momentum distribution is the one used successfully to explain proton-nucleus collision data.[5,6]

The scattering-angle, or the momentum-transfer, dependence of the QES cross sections are compared at the peaks of the solid curves shown by arrows in Fig. 7. The comparison at the peak is more appropriate than the tail of the curves because the θ_1 dependent shape is sensitively affected by the momentum distribution of nucleons inside the nucleus as well as the unaccounted rescattering processes. Reasonable fits of the single scattering calculation to the data were seen with one normalization. No visible anomalies of the QES in Ne+NaF collisions was observed.

Enhancements of the cross section, which is not related to QES, are seen at around θ_1=30° when θ_2<40°. These enhancements were not seen in the coplanar correlation function $C(P_1,\theta_1)$ but appears in Σ_d. The reason is as follows; Because the two-proton cross sections increase rapidly as θ_1 and θ_2 decrease, the Σ_d increases even if $C(P_1,\theta_1)$ slowly decreases. This enhancement of Σ_d are seen also in other sum energy region, namely E_s>500 MeV. It gives a contrast to the QES component in which enhancements were seen only in E_s=300 -500 MeV region. This type of correlation shows that the high-transverse momentum protons are associated with other protons with high-transverse

momentum which is emitted in the same plane and in the opposite side. At this moment, however, we have no theoretical explanation of this enhancement.

4. Ne + Pb data

Three distinct types of correlation were observed in the coplanar correlation function $C(P_1,\theta_1)$ of Pb target data. Firstly, when coincidence proton(p_2) were detected in low P_t regin at intermediate rapidity, Fig.3a, the correlations are very weak, $C(P_1,\theta_1)\approx 1.0$, in all kinematic region(Type I). It suggests that low P_t protons at intermediate rapidities are emitted almost isotropically around the beam axis. Secondly, when high-momentum coincidence protons were detected at forward angles, Figs.3b and 3c, $C(P_1,\theta_1)$ decreases down to 0.5 as P_1 increases(Type II). It is the same feature observed in ^{40}Ar+Pb collisions at 800 MeV/nucleon. It thus indicates the sideward emission of high-energy protons at forward angles also at 400 MeV/nucleon beam energy. Thirdly, a ridge of correlation($C(P_1,\theta_1)>1.0$) is seen, Fig.5a, when p_2 was detected at large angles(Type III). It is a type of correlations newly observed in heavy-ion collisions. It shows that the forward protons are associated with large angle protons which is emitted in opposite direction of the incident beam in the same reaction plane.

Combining these correlations observed in present experiment, the emission of the protons from the heavy-target collisions is azimuthally asymmetric with respect to the beam axis except in low P_t region at intermediate rapidity. The directions of asymmetries at forward angle high-momentum protons and at backward angle low-momentum protons are opposite. It is therefore the same effect shown by a plastic-ball experiment in which they observed the deviation of the symmetry axis of the particle emission from beam axis in Nb+Nb collisions.[4] They also showed that the polar angle of the symmetry axis become larger as the particle multiplicity increases.

The two-particle correlations of the Type II were analyzed by a hydro-dynamical model and a qualitative agreement was obtained between the model and the data.[2] In the frame work of the same model, the Type III correlation could be understood as the correlation between bounced projectile nucleons and the recoil target nucleon. In hydro-dynamical models, the bounce-off angles depend strongly on the impact parame-

ter as shown in Fig.8. On the other hand, because the target recoil nucleons are distributed widely at large angles, the distribution of these nucleons are rather insensitive to the impact parameter. When coincidence protons are detected at large angles, wide range of impact parameters are integrated. Then the bounced nucleons, distributed along the dashed line in Fig.8, produce a ridge in the correlation function. Hydrodynamical model was also used to understand the plastic ball data, and a qualitative agreement was also reported.

Since cascade models could not reproduce the asymmetric emission a year ago, it was thought that a hydro-dynamical behavior had been observed in high-energy nuclear collisions. Recently, however, revised cascade models,[7,8] which include nuclear potential and other nuclear effects, also show the asymmetric emission pattern. It, therefore, become difficult to say whether hydro-dynamical behavior is observed or not. Quantitative examinations of models are necessary to understand the mechanism of heavy-ion reactions. Our data show not only the asymmetric emission of the particles but also a new coplanar correlation between large angle and forward protons including momentum and angular relation Fig. 5a. The theoretical analysis to understand these momentum correlations is waited.

Summary

We have measured two-proton coincidence cross sections for 400 MeV/nucleon ^{20}Ne+NaF and ^{20}Ne+Pb collisions. A wide range of angles(θ=12-90°) and momenta(P=250-1200 MeV/c) was covered.

Coplanar correlation function of ^{20}Ne+NaF collisions showed a dominance of the quasi-elastic-scatterings (QES) of nucleons. Angular distributions of the QES were described reasonably well by the single scattering model. Enhancement of QES near the momentum transfer around 2-3m_π, which is predicted as a possible sign of the pionic instability, was not observed. An enhancement of the coplanar-type emissions were observed at high P_t region.

Coplanar-type correlation in ^{20}Ne+Pb data showed the asymmetric emission of forward going protons. Back-to-back correlations were observed between forward protons

and large angle protons. Data also showed the correlation between momenta of these protons. Hydro-dynamical models give qualitative understanding of observed correlations. However quantitative comparisons to Hydro-dynamical models as well as to other models, such as cascade models, are highly desirable in order to fully understand the reaction mechanism.

The present measurements have been carried out by the INS-LBL collaboration group at LBL, author gratefully acknowledges to those who participated the experiment; H. Hamagaki, S. Nagamiya, Y. Miake, S. Schnetzer, Y. Shida. This work was supported by the Director, Division of Nuclear Physics of the Office of High Energy and Nuclear Physics of the US Department of Energy under contract DE-AC03-76SF00098, the INS-LBL Collaboration Program, and by the US-Japan Joint Program for High-Energy Physics. The author would like to give thanks to the Yamada Foundation for their support.

References

(1) I. Tanihata, M.-C. Lemaire, S. Nagamiya, and S. Schnetzer, Phys. Letters 97B (1980) 363.

(2) L. P. Csernai, W. Greiner, H. Stocker, I. Tanihata, S. Nagamiya, and J. Knoll, Phys. Rev.C 25 (1982) 2482.

(3) J. Gylassy and W. Greiner, Annals of Physics 109 (1977) 485.

(4) H. A. Gustafsson, H. H. Gutbrod, B. Kolb, H. Lohner, B. Ludewigt, A. M. Poskanzer, T. Renner, H. Riedesel, H. G. Ritter, A. Warwick, F. Weik, and H. Wieman, Phys. Rev. Letters 52 (1984) 1590.

(5) I. Tanihata, S. Nagamiya, S. Schnetzer, and H. Steiner, Phys. Letters 100B (1981) 121.

(6) Y. Miake, H. Hamagaki, S. Kadota, S. Nagamiya, S. Schnetzer, Y. Shida, H. Steiner, and I. Tanihata, to be published

(7) Y. Kitazoe, M. Sano, Y. Yamamura, H. Furutani, and K. Yamamoto, Phys. Rev.C 29 (1984) 828. Y. Kitazoe, H. Furutani, H. Toki, Y. Yamamura, S. Nagamiya, and M. Sano, Phys. Rev. Letters 53 (1984) 2000.

(8) J. Cugnon ,Talk given at this conference.

Figure Captions

Fig.1 Geometry of the coincidence measurement.

Fig.2 Experimental setup.

Fig.3 Contour line representation of the coplanar correlation function, $C(P_1,\theta_1)$, for forward proton coincidence($20<\theta_2<40°$) in rapidity(Y)-P_T/m_p plane. Corresponding laboratory angles are also shown for convenience.

Fig.4 Coplanar correlation function, $C(P_1,\theta_1)$, for coincidence protons for $50°<\theta_2<70°$.

Fig.5 Coplanar correlation function, $C(P_1,\theta_1)$, for large angle proton coincidence ($75°<\theta_2<85°$).

Fig.6 Emission pattern and the coplanarity.

Fig.7 Difference cross section Σ_d between in-plane and out-of-plane coincidence. Solid curves show results of single scattering model calculations. The observed QES cross sections and the model calculations are compared at the center of the QES kinematics which are indicated by arrows. Reasonable agreements are seen.

Fig.8 Relation between bounce-off angle, momentum, and impact parameter of the collisions.

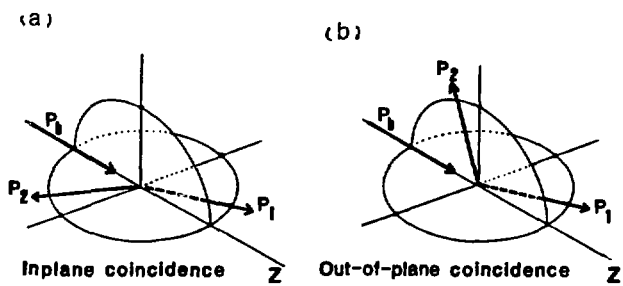
(a)
(b)
P3
P2
P1
P3
P2
P1
Inplane coincidence
Z
Out-of-plane coincidence
Z

Fig. 1

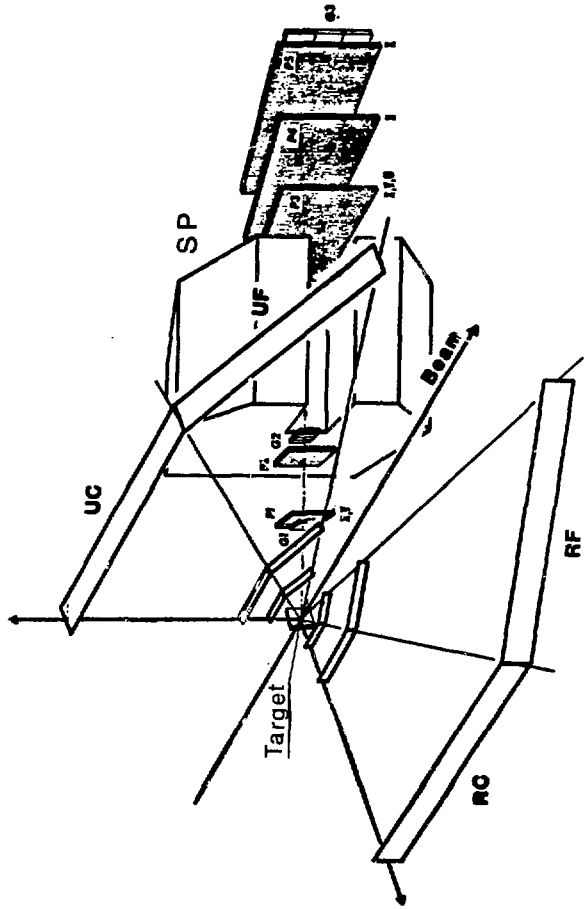

FIG. 2

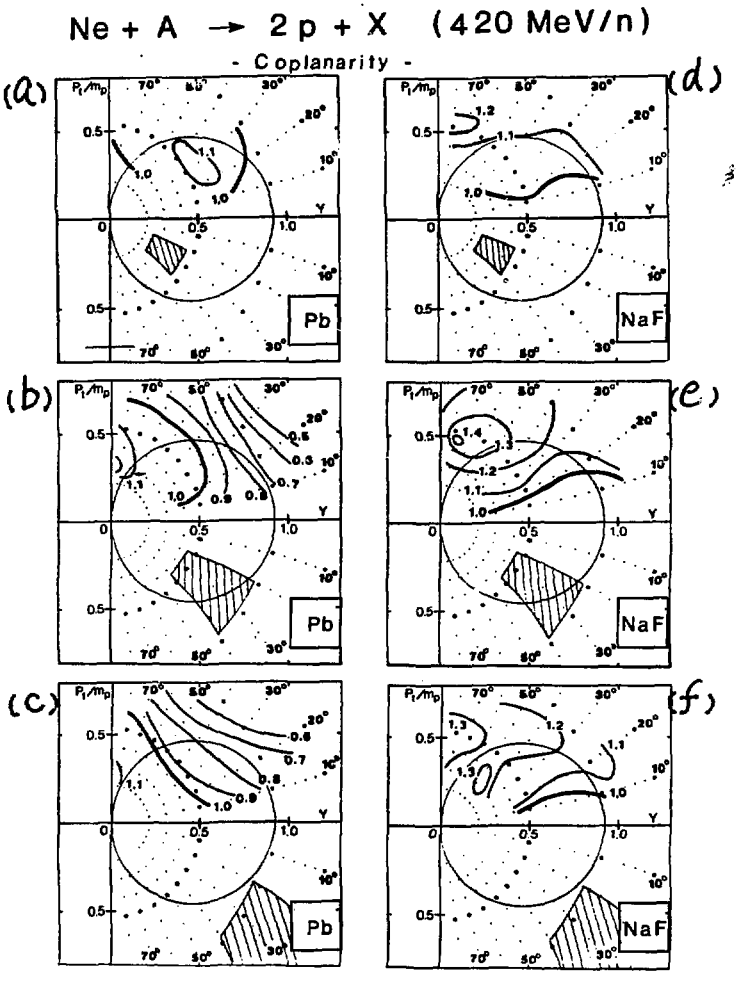
Ne + A → 2p + X (420 MeV/n)
- Coplanarity -
(a)
(b)
(c)
(d)
(e)
(f)
Pb
NaF
Y
P⊥/mp
70°
50°
30°
20°
10°
0
0.5
1.0
1.1
1.2
1.3
1.4
0.9
0.8
0.7
0.6
0.3
XBL 849-3859

FIG. 3

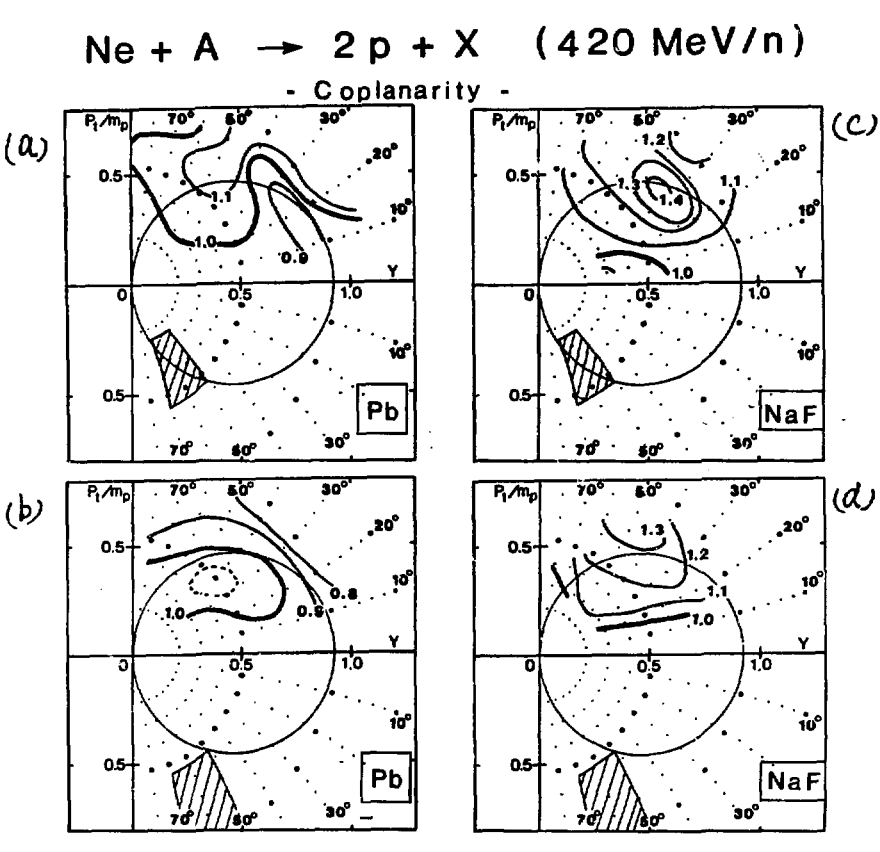

FIG. 4

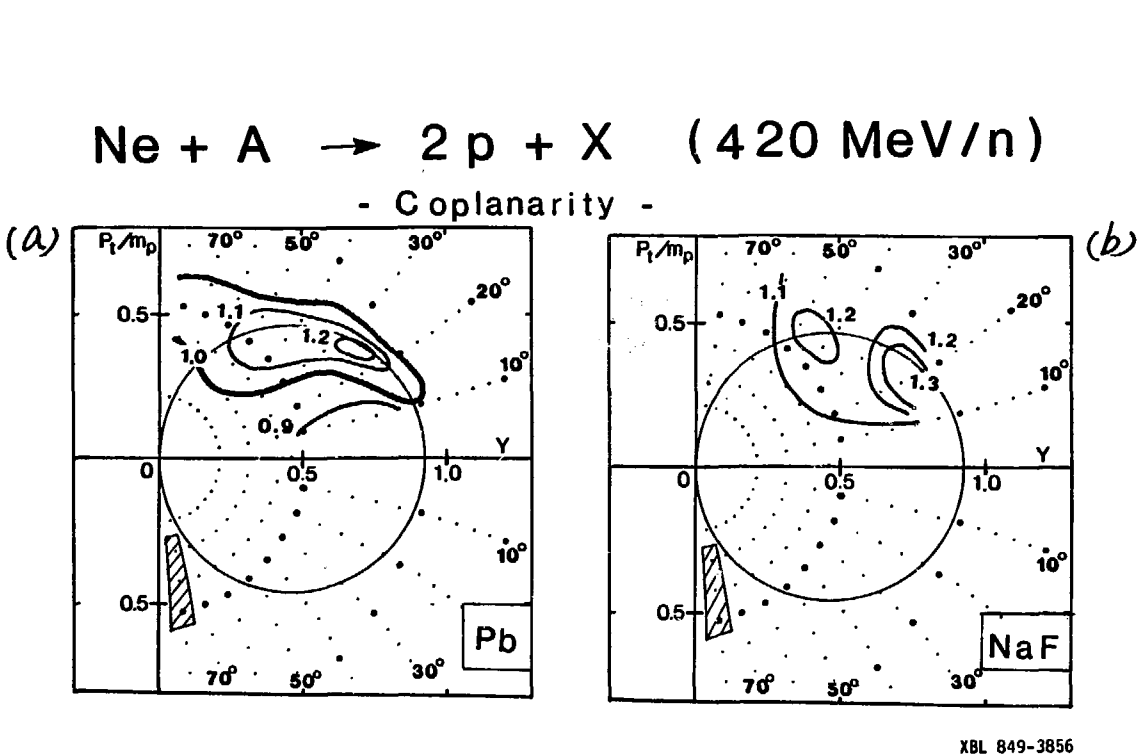
Ne + A → 2p + X (420 MeV/n)
- Coplanarity -
(a)
(b)
P_t/m_p
70°
50°
30°
20°
10°
0.5
1.1
1.2
1.0
0.9
Y
0
0.5
1.0
Pb
NaF
1.3
XBL 849-3856

FIG. 5

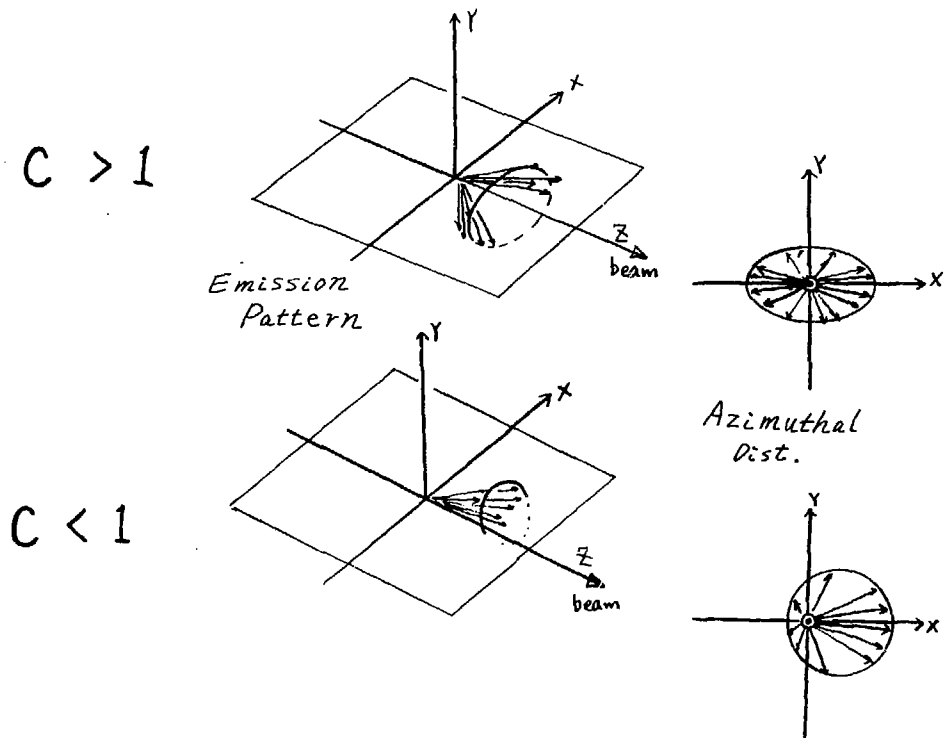
C > 1
Y
X
Z
beam
Emission
Pattern
Y
X
Azimuthal
Dist.
C < 1
Y
X
Z
beam
Y
X

FIG. 6

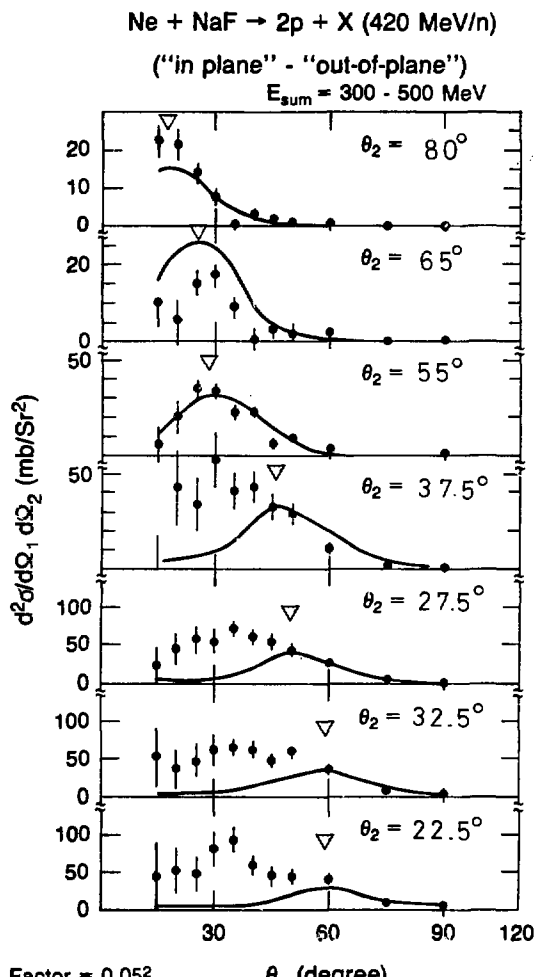

FIG. 7

XBL 849-10860

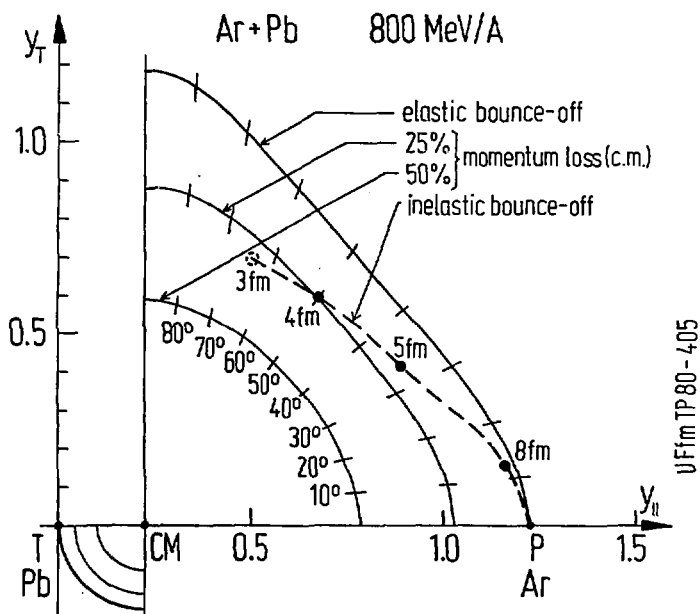
Ar+Pb 800 MeV/A
y_T
1.0
0.5
elastic bounce-off
25%
50%
momentum loss(c.m.)
inelastic bounce-off
3fm
4fm
5fm
8fm
80°
70°
60°
50°
40°
30°
20°
10°
T
Pb
CM
0.5
1.0
P
Ar
1.5
y_{II}
UFfm TP80-405

FIG. 8